Journal of Aerosol Science 51 (2012) 35–48

Contents lists available at SciVerse ScienceDirect

Journal of Aerosol Science

journal homepage: www.elsevier.com/locate/jaerosci

Characterization of multi-jet electrospray systems

C.N. Ryan [a,1], K.L. Smith [b], J.P.W. Stark [a,*]

[a] Department of Engineering, Queen Mary University of London, London E1 4NS, UK
[b] School of Mechanical, Aerospace and Civil Engineering, the University of Manchester, Manchester, M13 9PL UK

ARTICLE INFO

Article history:
Received 29 November 2011
Received in revised form
28 February 2012
Accepted 28 March 2012
Available online 14 April 2012

Keywords:
Electrospray
Multi-jet
Minimum flow
Charge efficiency

ABSTRACT

Experimental results obtained in multi-jet mode electrospray are presented for two fluids: propylene carbonate and triethylene glycol, each doped with sodium iodide. No structural features were provided in the electrospray emitting capillary in order to stabilize the multi-jet process. For a low number of jets emitted the meniscus is not bound to the rim of the capillary; however as the number of jets increases the mode becomes the so-called rim-mode electrospray. The data thus obtained shows that in all cases the relationship between current and flow rate observed in single cone-jet mode is maintained in multi-jet mode when the current and flow rate is normalized by the number of jets. The results were obtained here for a range of capillary external diameter and under either vacuum or atmospheric pressure; neither of these aspects influenced the observed relationships. The high accuracy flow metering system used demonstrates that in the multi-jet modes the minimum stable flow rate per cone-jet system is reduced below that observed in the single cone-jet mode. However multi-jet mode is seen to be less stable, in that each jet in multi-jet mode is unable to support the same volumetric flow as in the single jet mode; indeed it appears that there is a maximum total flow that can be maintained in an electrospray, independent of the number of jets through which the flow is achieved. A simple model is presented that links these observations to predict the maximum number of jets that may be obtained in the type of multi-jet processes observed here.

1. Introduction

Electrospray phenomena have intrigued scientists for over 100 years, with many detailed features of their operation still not fully understood (Fernández de la Mora, 2007). Following Rayleigh's, 1882 prediction that a drop charged beyond a certain limit would loose charge by ejecting a charged stream of fluid (Rayleigh, 1882), a systematic investigation by Zeleny in a series of 3 papers, revealed the richness of phenomena associated with what we now term electrospray (Zeleny, 1914, 1915, 1917).

It was in the second of Zeleny's papers published in 1915 that the first recorded reference to multi-jet phenomena was made. In those experiments alcohol was sprayed in atmospheres of either air or carbon dioxide and it was observed: "*for voltages well above that for which the steady conical surface changed into a blurred agitated one, the appearance became*

* Corresponding author. Tel.: +44 207 882 8875.
E-mail addresses: c.n.ryan@qmul.ac.uk (C.N. Ryan), kate.smith@manchester.ac.uk (K.L. Smith), j.p.w.stark@qmul.ac.uk (J.P.W. Stark).
[1] Tel.: +44 207 882 5262.

0021-8502/$ - see front matter © 2012 Elsevier Ltd. All rights reserved.
http://dx.doi.org/10.1016/j.jaerosci.2012.03.007

(*with reference to a figure…*) *a number of fine points with their attendant dark streaks arranged along the circumference of the raised edge*".

Taylor (1964) set down a mathematical framework for the conical structure observed for perfectly conducting liquids, it was not until 1989 that Cloupeau and Prunet-Foch (Cloupeau & Prunet-Foch, 1989) characterized the variety of modes that are seen as the electrostatic conditions are changed between the fluid carrying capillary and an external electrode plate. It is this broad categorization that is now used throughout the literature to reference the individual modes.

Of these modes the one that has been subjected to most detailed study has been the cone-jet mode. A number of different scaling laws have been derived for this mode of operation (Fernández de la Mora & Loscertales, 1994; Gañán-Calvo et al., 1997; Gañán-Calvo, 2004) and a review of these together with a broader review may be found in (Fernández de la Mora, 2007). Cone-jet mode is the most stable of the modes and has been used in a variety of applications, but most especially as an ionization method of large molecules for analysis by mass spectrometry in ES-MS (Kebarle & Verkerk, 2009). It has also been considered for use in colloid-electrospray electric propulsion for spacecraft (Alexander et al., 2006; Gamero-Castaño, 2001; Martinez-Sanchez & Pollard, 1998).

At a voltage below that required to obtain steady cone-jet a variety of pulsation modes may be observed (Juraschek & Röllgen, 1998). A number of these pulsation modes have been investigated in some detail as a method for isolating discrete volumes of fluid that may be deposited via drop-on-demand techniques, akin to inkjet printing facilitating surface modification and additive manufacturing processes (Paine et al., 2007).

The mode however that has perhaps been studied least is the multi-jet mode wherein from the same meniscus several stable jets may be emitted simultaneously. In the original paper by Cloupeau & Prunet-Foch (1989), two distinct variants of this mode were identified and are reproduced in Fig. 1 (their Figure 2) showing two distinctly different aspects.

Fig. 1a and b relate to the cone-jet mode discussed previously, which often becomes less axisymmetric as the applied voltage is increased. Fig. 1c is the topology having the emission of multiple jets from the main meniscus itself, in the case shown with two jets. In contrast Fig. 1d, a condition achieved at higher electrical stress, as originally noted by Zeleny, the fluid meniscus recedes essentially to the capillary exit and multiple jets appear to form from a film of liquid over the capillary surface. In subsequent papers researchers have termed both these to be multi-jet modes, although the mode associated with Fig. 1d has also been identified as rim-mode electrospray by some authors.

A number of papers include images of the highly stressed meniscus as shown in Fig. 1d (Cloupeau & Prunet-Foch, 1994; Hayati et al., 1987; Hendricks et al., 1964; Jaworek & Krupa, 1996; Jones & Thong, 1971; Lüttgens et al., 1992; Marsh et al., 1988; Shtern & Barrero, 1994; Thong & Weinberg, 1971; Yoon et al., 2001). Recently more detailed characterization of this mode has been given, with the most extensive reports given by Noymer & Garel (2000), Duby et al. (2006) and Gu et al. (2005, 2010). Whilst Gu et al.'s configuration is somewhat different in detail all these investigations were undertaken using relatively large capillaries, typically approaching 1 mm in diameter, and in Duby's research the capillary surface was grooved to enhance the stability of the multi-jet process, whilst the operational flow rates were relatively high $\sim$10 μl/s. Noymer and Garel found that the mean droplet size in multi-jet mode was approximately one third that found in cone-jet mode for a given liquid flow rate (Noymer & Garel, 2000). Although Duby et al. did not directly compare their results with those of Noymer and Garel, they found that the relationship between spray current and flow rate Q was similar in multi-jet mode to that in cone-jet mode, a finding which seems to be at variance with the earlier findings. Gu et al. have studied multi-jets in insulating liquids and at fixed flow rate found that the current increased in proportion to the square of the applied voltage. For each of these investigations into highly stressed multi-jet electrospray the fluids were of low conductivity, between 1 and 10 μS/m with associated high flow rate $\sim$0.1–10 μl/s. In all of these reported experiments cited, the flow rate into the capillary was controlled by a syringe pump to maintain a constant flow. The investigation of multi-jet phenomena has also been extended to coaxial electrospray by (Park et al., 2011), which again identified the use of a grooved surface to aid multi-jet stabilization and where fluids were controlled by syringe pumps.

Topologically there is quite a distinction between the two multi-jet variants shown in Fig. 1c and d, whether or not the underlying electrospray phenomena are indeed distinct. Thus far however there appears to have been no characterization of the type of multi-jet mode shown in Fig. 1c; this paper presents data covering both these modes. The experimental configuration that we have adopted is different from the previous multi-jet/rim mode papers but is more similar to the

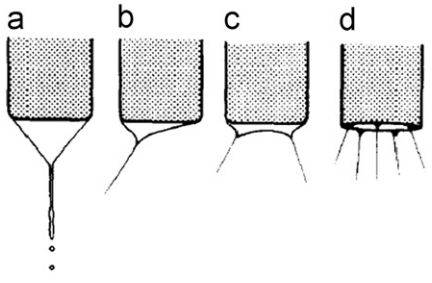

Fig. 1. Reproduced from Cloupeau & Prunet-Foch (1989): (a) cone-jet mode, (b) loss of axial symmetry in cone-jet mode, (c) two emissive cups, (d) multiple emission sites from capillary rim.

approach used by many others studying cone-jet processes such as (Fernández de la Mora & Loscertales, 1994), in that rather than using a syringe pump to control the flow we have used a pressure head to maintain constant upstream conditions. As a result the fluid in the electrospray responds to the effects of changing external electrostatic conditions with a change in flow rate. This feature of flow rate sensitivity to voltage has been documented previously by our group (Alexander et al., 2007; Ryan et al., 2009; Ryan, Unpublished; Smith et al., 2006b). Using the same high precision flow meter as in these earlier reports and operating under a constant pressure head with an associated steady fluid jet or multi-jet in the cases reported herein, flow rate sensitivity at the level of 0.1 nl/s is achieved. This flow sensitivity is essential to capture accurately the low flow rates reported here.

2. Experimental procedure

Two different configurations were adopted to investigate the multi-jet electrospray performance characteristics. Key elements of these configurations were common, viz. the flow meter and constant static pressure head; the main difference between the experimental configurations was that some experiments were carried out in air, whilst others were carried out under vacuum.

2.1. Electrospray measurements at atmospheric pressure

The equipment used for atmospheric experiments is that used previously (Ryan et al., 2009). As illustrated in Fig. 2, it consists of an electrospray system, using a stainless steel emitter supplied with the electrospray fluid and an extractor electrode (with an aperture) to which the high voltage was attached. A secondary electrode is used to collect the sprayed fluid after it had passed through the extractor electrode aperture. Both the emitter and the secondary (collector) electrode were connected to ground. A known negative voltage was applied to the extractor electrode, using a FUG HCL 14–6500 power supply, with the high voltage controlled by LabView software, via an NI USB-6008 DAQ card.

The spray current was determined by measuring the current flow on the emitter (at virtual earth) rather than the downstream collector, in order to ensure that the total spray current was identified. This current was determined from the voltage drop across a 1 MΩ resistor. An ISO-TECH IDM 207 multimeter logged the resulting voltage drop at a frequency of 2 Hz.

In these atmospheric measurements the size of the capillary internal and external diameter was varied; 11 different capillary types were used. The emitter internal diameter was varied from 100 to 635 μm with a constant external diameter of 810 μm (with specific internal diameter values of 144, 184, 266, 350, 465 and 644 μm). The external diameter was varied from 200 to 1610 μm; these capillaries had a nearly constant mean internal diameter of 125 μm, but in detail varied from 100 μm to 150 μm. The process by which the diameters were determined is given in full by (Ryan et al., 2009; Ryan, Unpublished). Each capillary used had a smooth, flat exit surface at 90° to the tube wall.

The high accuracy in-line flow rate measurement system developed during our previous investigations into electrospray phenomena was used upstream of the emitters. A complete description of the instrument is provided elsewhere (Smith, 2005). The flow measurement is achieved by determining the pressure drop between a pair of high precision, absolute pressure transducers, over a section of the fluid feed pipe-work. The transducers selected are temperature compensated Paroscientific Digiquartz 740-23A quartz crystal pressure transducers. The absolute accuracy of these is 0.01% full scale and a maximum resolution of 1 ppm at a sampling rate of ~1 Hz.

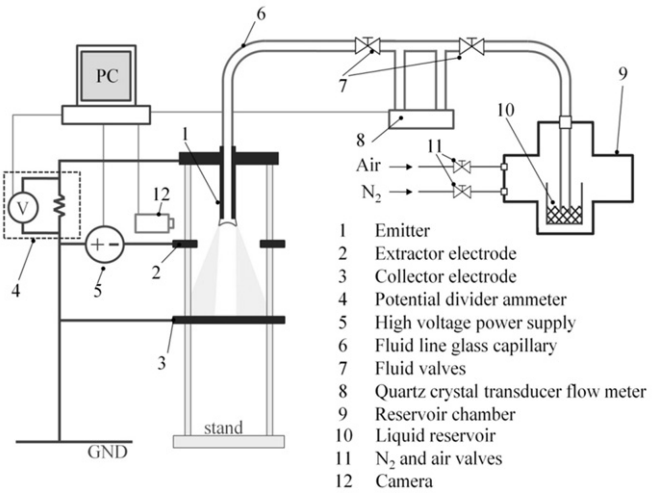

Fig. 2. Representation of electrospray setup, for atmospheric testing.

In steady flow the measured pressure drop, ΔP, is directly proportional to the volumetric flow rate Q as described by the Poiseuille equation

$$Q = \frac{\Delta P \pi {r_i}^4}{8 \mu L} = \frac{\dot{m}}{\rho}. \quad (1)$$

where $\dot{m}$ is the mass flow rate, ρ is the fluid density, μ is the fluid viscosity, r_i is the internal radius of the pipe section and ΔP is the pressure change along length L of the pipe.

The resolution of the pressure difference is proportional to the hydraulic impedance between the transducers. In these experiments the measurement section had internal radius of 0.125 mm and length 0.5 m; this selection results in a flow rate resolution of 0.1 nl s^{-1}. The flow rate was calibrated using the method used previously (Smith, 2005), where the mass output was collected over a certain period of time, with the pressure difference across the two transducers measured.

A nominal flow rate (in the absence of an applied electric field) was set by varying the reservoir height above the exit plane of the capillary. The large internal diameter of the reservoir and the very low flow volume dispensed during experiments ensured that a constant pressure head was maintained. The high voltage was varied by the PC controlled power supply and set to increase incrementally following the onset of cone-jet mode. The size of the voltage steps varied between 30 and 200 V. The voltage was only increased after sufficient time for steady state electrospray to be established and recorded.

2.2. Vacuum based measurements

The vacuum based measurements were obtained from an experimental setup very similar to the configuration described and used for atmospheric experiments. This included the application of the high resolution flow meter described above, but rather than using a fused silica capillary between the transducers, a custom made inert glass lined tubing GLT™ from SGE Ltd was used. This design minimizes the use of unions and connectors, reducing the number of potential leakage sites for the ingress of air into the system.

The electrospray emitter and counter electrode assembly only were housed in a vacuum chamber. This chamber was evacuated down to a pressure below 10^{-3} mbar during testing using a turbo molecular pump backed by a roughing pump.

The emitter used was a stainless steel Cooper's capillary, with an internal diameter of 305 μm and an external diameter of 560 μm. This capillary also had a smooth exit surface as in the atmospheric measurements.

Unlike the atmospheric experiments, the counter electrode was a simple plane disk with no aperture. A positive high voltage was applied by a Canberra model 3105 to the emitter, rather than a negative voltage to the extractor as with atmospheric experiments.

The current on the emitter and extractor electrode were measured on-line by a custom built two stage optically isolated system (Aplin et al., 2008). This approach safely converted the signal from high voltage to a data logger at ground potential. A battery powered high voltage stage, floated at the same potential as the emitter, contains a current to voltage converter in the transresistance configuration. This converter is then followed by a voltage to frequency converter for optical signal transmission. A fibreoptic cable connected to a frequency to voltage converter chip at ground potential comprises the second stage, which is then directly and safely connected to a PC for data logging. This system was designed to measure currents up to ± 2 μA, with a voltage response of ~ 1 mV/nA and a time response of 1 s. The spray current measurement data presented below is again that determined on the emitter in order to ensure that the total spray current is detected. As a result whilst there are small differences in the electrical configuration between the atmospheric based and vacuum based measurements, the results are directly comparable.

2.3. Electrospray solutions

For experiments conducted in atmospheric conditions, Propylene Carbonate (PC1 solution) was chosen as the electrospraying solvent, doped with Sodium Iodide to a conductivity of 2.6×10^{-3} S m^{-1}.

A lower vapor pressure fluid was required to be used in the vacuum experiments. Triethylene Glycol was chosen, again doped with Sodium Iodide to give two conductivity values, TEG100: 1.0×10^{-2} S m^{-1} and TEG160: 1.6×10^{-2} S m^{-1}.

The properties of the solvents are given in Table 1.

Table 1
Solution properties.

Solution	Concentration (mol/L)	Conductivity (S/m)	Density (kg/m^3)	Viscosity (N/sm^2)
TEG100	0.083	0.010	1123.5[a]	0.049[a]
TEG160	0.167	0.016	1123.5[a]	0.049[a]
PC1	0.007	0.003	1206.9[b]	0.028[b]

[a] Viscosities and densities listed are those of the base solvent given in Riddick et al. (1986).
[b] Viscosities and densities listed are those of the base solvent given from Beyer et al. (1987) Naejus et al. (1997). All properties obtained at 20 °C.

3. Multi-jet electrospray results

3.1. Current flow rate dependence in multi-jet

Fig. 3 shows typical responses of flow rate and current as the applied voltage between the fluid and ground plane increases. Data is shown for experiments using the PC solution. Current is shown in a continuous fashion whilst flow rate has been averaged at each voltage increment. For all the data reported in this paper voltage was increased (rather than decreased) during each experiment run. Responses were obtained with the voltage decreasing and demonstrated that in multi-jet mode hysteresis is apparent, as has been described with cone-jet mode (Cloupeau & Prunet-Foch, 1989; Fernández de la Mora, 2007; Smith, 1986). However we make no further reference to this observation in this paper.

Within stable cone-jet mode as the voltage is increased both the flow rate and the current respond. The detailed sensitivity of the flow rate dependency on voltage to geometric configuration in cone-jet mode electrospray has been evaluated in depth (Ryan et al., 2009) and demonstrated that the flow rate dependence is broadly linear with applied voltage.

At some applied voltage the single cone-jet bifurcates into two jets with an associated step change in current. For the data presented in Fig. 3 this occurs at ~4.4 kV. In Fig. 3 this current increase occurs in one large step, whilst in some cases the current goes through an intermediate state at the onset of multi-jet mode, corresponding to some instability. This transition type instability occurred more frequently at higher nominal flow rate.

Depending upon the stability of the transition from n-jets to $n+1$-jets the total flow rate may either slightly reduce, or increase, but in each case only to a small extent. This may be due to the effect of space charge, which is the likely explanation of the decrease in flow rate sometimes observed when going from pulsed to cone-jet mode (Ryan et al., 2009). Once stability in the multi-jet mode is established the flow rate and current continue to increase linearly and with very similar sensitivity to voltage as in the cone-jet mode.

Fig. 4a shows an image of a two cone-jet system showing the typical topology of the multi-jet phenomena we have studied. It bears a strong resemblance to Fig. 1c, with individual jets clearly apparent and emanating from the meniscus directly. At higher voltages further cone-jets are formed, as shown in Fig. 4b with an appearance more like Fig. 1d. Each further cone-jet system resulted in another large increase in current, with little change in the flow rate.

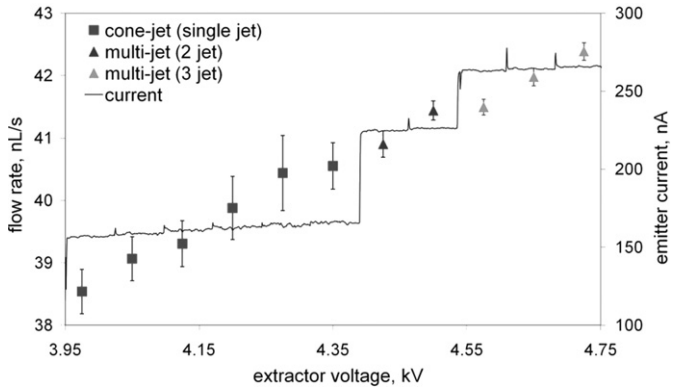

Fig. 3. Flow rate and current sensitivity to voltage for an electrosprayed solution PC (see Table 1) on a capillary having an internal diameter 125 μm and external diameter 230 μm.

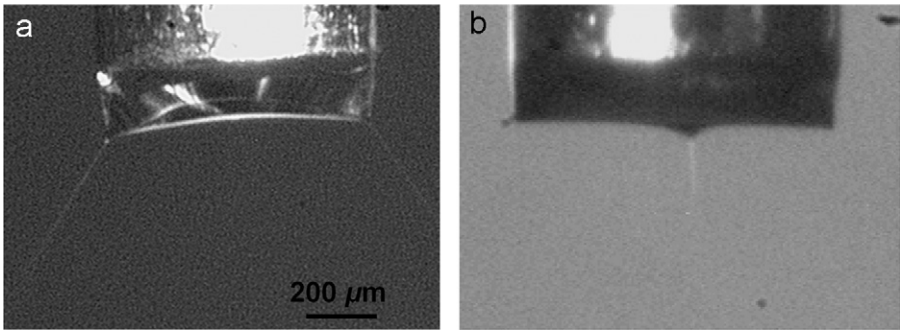

Fig. 4. Images of typical multi-jet electrospray observed, (a) a two cone-jet electrospray and (b)a rim-jet mode multi-jet with three cone-jets observed.

Using solution PC1 over 150 experiments were carried out using capillaries of varying internal and external diameter. In each experiment a constant flow was established initially, in the absence of an applied voltage by variation of the pressure head of the reservoir; we term this initial flow to be the "nominal flow rate". As the voltage was applied and then increased in steps as described in Section 2, the electrospray went through a series of transitions with between 1 and 4 jets observed. In this paper we term each of these as an *n-jet* mode, where *n* is the number of jets observed. From each data set it is possible to identify the onset voltage (i.e. the lowest voltage for stable electrospray) for a given total flow rate (the initial flow rate plus voltage induced flow rate). Fig. 5 plots the current at voltage onset for each multi-jet mode as a function of the onset flow rate.

If it is assumed that each jet carries an equal portion of both the total flow and the total current, it is possible to overlay the data for the individual current/flow rate relationship as the number of jets increases. This data is plotted for solution PC1 in Fig. 6. The data plotted in this way shows a collapse onto a single curve for the different jet modes carrying the electrospray fluid. It is notable in this data that whilst there is some scatter, the overall coefficient of determination is 0.97.

It would therefore seem that in these experiments the $I(Q)$ relationship is independent of the number of jets, and can be directly compared to the cone-jet relationship. This comparability of the $I(Q)$ multi-jet data has been described before for

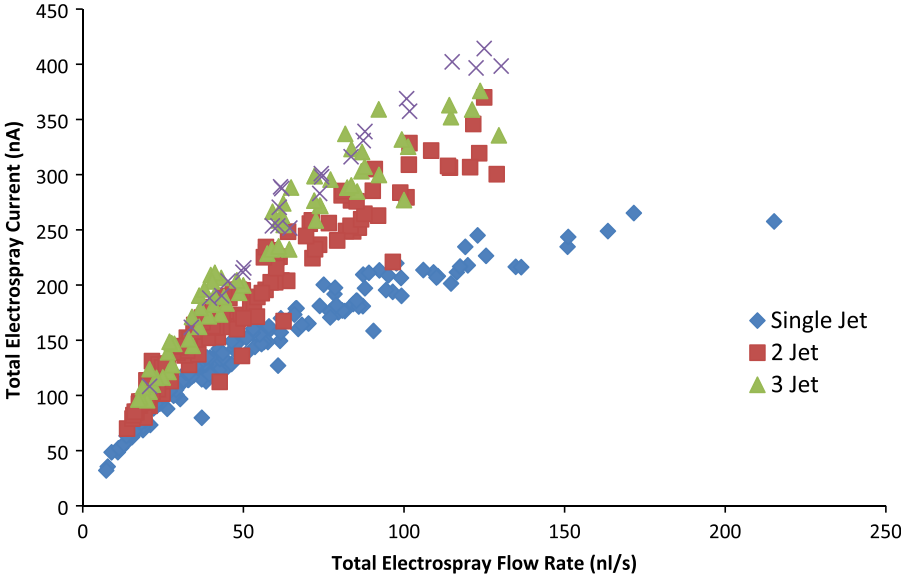

Fig. 5. Total current as a function of total flow rate for all sprays obtained with fluid PC1.

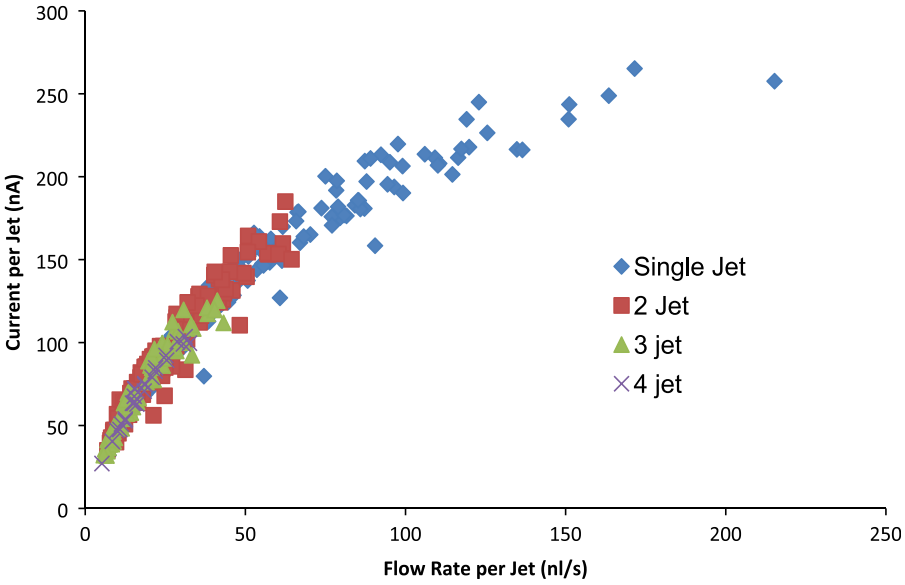

Fig. 6. Dependence of current carried per jet as a function of flow rate per jet for the fluid PC1.

the multi-jet rim-jet mode (Duby et al., 2006), although we note that in Duby's experimental configuration emitter tip rim was etched with channels in order to stabilize the multi-jet jet source position.

The new data set reported here was obtained with 11 different capillary sizes having a range of both internal and external diameter values. The observation that all the recorded data collapses in the way shown in Fig. 6 indicates that the effect of the capillary dimensions in multi-jet mode has little influence on the functional relationship between spray current and flow rate. This has been noted previously in the case of single cone-jet mode by (Fernández de la Mora & Loscertales, 1994).

The flow characterization of the triethylene glycol solutions (TEG160, TEG100) were carried out in a similar manner to the PC1 solution tests. The current flow rate data for these solutions showed similar trends to the data plotted in Fig. 6, in that the normalized current per jet as a function of the flow rate per jet appears to collapse, albeit with a different value of the best fit power law parameters, with the differing solution properties (Smith et al., 2006a).

Many authors have adopted the dimensionless scaling laws identified either by (Fernández de la Mora & Loscertales 1994) or (Gañán-Calvo et al. 1997, 2004). These scaling laws were developed for single cone-jet mode. In the scaling laws of Fernandez de la Mora the non-dimensional flow rate η and the non-dimensional current ξ are given by

$$\eta = [\rho K Q/\gamma \varepsilon \varepsilon_0]^{1/2}, \quad \xi = \frac{I}{\gamma(\varepsilon_0/\rho)^{1/2}} \tag{2,3}$$

where K is the fluid conductivity, γ is the surface tension, ε is the relative permittivity, and ε_0 is the permittivity of free space. It has been found that by plotting $\xi/f(\varepsilon)$ against η, where $f(\varepsilon)$ is an empirical function of ε, that single cone-jet mode current and flow rate data using different polar solvents collapses.

The multi-jet data, excluding the single cone-jet mode obtained for the PC1, TEG100 and TEG160 solutions, is plotted in this format in Fig. 7. The PC1 data is for up to 4 cone-jets in multi-jet mode, whilst the TEG data is for up to 6 cone-jets. Dimensionless current and flow rate per jet is plotted, with the dimensionless current divided by the empirical function $f(\varepsilon)$. It is apparent from this that whilst there is an overall trend captured by this procedure, there is still some significant scatter in the data, when plotted in this way.

3.2. Stable flow rate range and voltage effects in multi-jet electrospray

As described in Section 2 the individual electrospray data was obtained by (i) establishing a nominal flow through the capillary; (ii) increasing the voltage until stable cone jet was observed, (iii) continuing to increase the voltage whilst noting the onset I, Q, and V conditions for the appearance of each additional jet. Throughout this process the pressure head remained constant.

Following from the way the data collapses under the assumption of equal current and flow rate through each jet (shown in Fig. 6) we shall forthwith assume that the flow is indeed so divided between the number of jets. We shall therefore refer to the flow rate per jet in an n-jet mode in the form Q_n and the total flow through the electrospray in an n-jet mode as Q_n^{total}, with

$$Q_n = Q_n^{total}/n \tag{4}$$

An estimate of the minimum stable flow rate, Q_{min} predicted on the basis of empirical observations of $Q_{\min} = \gamma \varepsilon \varepsilon_0/\rho K$ (Fernández de la Mora & Loscertales, 1994), identifies that for PC1 this minimum flow is of the order of 7.5 nL/s. An investigation of the minimum flow rate was therefore undertaken for this fluid in the multi-jet mode by reducing the nominal flow rate to establish the ultimate minimum flow stability. Due to the low predicted minimum flow rate in the TEG solutions, of the order 0.5 nL/s for the most conductive solution, no systematic attempt at determining the minimum flow rate in the TEG solutions was attempted.

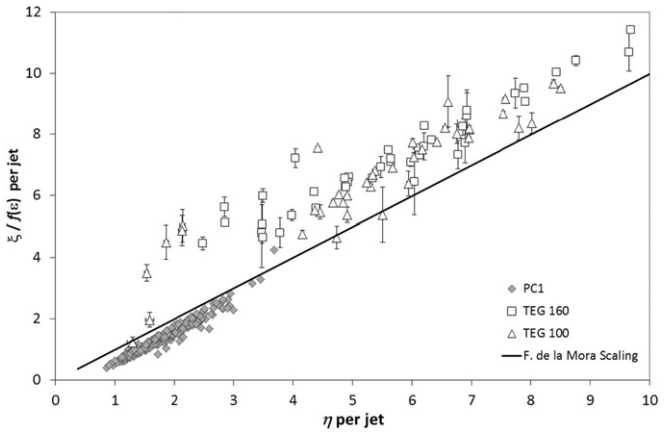

Fig. 7. Multi-jet data of $\xi/f(\varepsilon)$ against η for all trial solutions tested.

Table 2
Minimum flow rate per jet (nL/s) observed for solution PC1 as a function of the number of jets.

Fluid	1-jet $Q_{1(\min)}$	2-jet $Q_{2(\min)}$	3-jet $Q_{3(\min)}$	4-jet $Q_{4(\min)}$	$Q_{1(\min)}$ predicted
PC1	7.3	6.9	5.8	5.2	7.5

Table 3
Maximum total flow rate $Q_{\max}^{total}$ (nl/s) observed.

Fluid	1 jet (nl/s)	2 jet (nl/s)	3 jet (nl/s)	4 jet (nl/s)	5 jet (nl/s)	6 jet (nl/s)
PC1	305.7	230.2	171.6	171.9	–	–
TEG160	121.3	98.7	121.4	99.1	120.7	121.8
TEG100	162.0	121.9	162.6	163.2	118.7	162.5

The minimum flow rate at which stable cone-jet and multi-jet electrospray operation in PC1 is reported in Table 2. In this table each of the flow rate values are the flow per jet $Q_{n(min)}$. We note firstly that the value of $Q_{1(min)}$, i.e. the minimum flow rate in single cone-jet mode, is consistent, within the measurement accuracy (0.1 nl/s) to the scaling law prediction on minimum flow rate. Secondly we observe there to be a reducing minimum flow rate as the number of jets increases. This reduction is statistically significant and is well fitted by a linear trend. The resulting low flow rate data are indeed those data points plotted in Fig. 7, having values of dimensionless flow rate below unity; only one single cone-jet result fell below this limit.

It should be noted that the results in Table 2 present the minimum flow rate per jet that was seen to be stable in each of the multi-jet modes. Therefore they include the voltage-induced flow rate, as illustrated in Fig. 3.

If we consider the total maximum flow rate that was stably sprayed through the electrospray process; this is identified to be $Q_{\max}^{total}$. This *total* flow is thus the sum of all jet contributions over the number of jets n, comprising the particular multi-jet mode. Table 3 identifies this maximum *total* flow rate measured for each of the fluids tested.

The data obtained with PC1 solution was obtained with a variety of capillaries having various external diameters. It was found that the higher flow rates were achieved on the larger diameter capillaries. It is indeed data from the largest diameter capillary (1.61 mm) that is therefore included in Table 3 for the PC1 solution and for this capillary there is a decreasing value of maximum flow as the number of multi jets increases. All the TEG data were obtained from a capillary having a significantly smaller outside diameter (560 μm). Whilst there is some scatter in the TEG solutions reported in Table 3 for the value of $Q_{\max}^{total}$, there is a suggestion that for this data there may be a maximum total flow rate that can be carried in the electrospray, independently of the number of jets through which this flow is sprayed. The consequence of both these observations is that it is inevitable, but not perhaps surprising that the maximum stable Q that flows through each separate cone-jet system in multi-jet mode decreases as the number of jets increase. This observation is also evident from Fig. 6, where the $I(Q)$ data becomes more focussed towards lower flow rates as the number of cone-jets increases. However this reducing stability as the electrospray becomes more electrically stressed does not naturally lead to the suggestion of a fixed maximum flow through the entire electrospray process.

We have examined each individual experimental data set to identify for each *nominal* flow rate how the *onset* flow rate $Q_{n(on)}$ changes as a new jet emerges signaling a jet mode change. In this we wish to make a distinction between *onset* flow $Q_{n(on)}$ for a particular mode and the *minimum* flow $Q_{n(min)}$ in the same mode. Minimum flow rate is the lowest flow rate that it is possible to operate a stable electrospray. This is associated with the minimum flow rate first highlighted by Fernández de la Mora & Loscertales (1994) as an empirical observation; this minimum flow rate always will be initiated at a minimum voltage, since any increase in voltage will increase the flow rate unless there is a flow control mechanism in place, such as a syringe pump feed system. Historically this minimum has been defined only with regard to single cone-jet mode, although the results of Table 2 extend this to multi-jet modes. The minimum flow rate is associated with the smallest value of nominal flow leading to stable electrospray: a quoted value for $Q_{n(min)}$ thus is the sum of two components the nominal flow rate and the electrically induced flow rate.

In contradistinction, the onset flow $Q_{n(on)}^{total}$ is the total flow rate through the electrospray observed when the n-jet mode is first observed, for each nominal flow rate investigated. Again this flow rate is the sum of two components – the nominal flow rate and the electrically induced flow rate. Since the minimum flow rate in single cone-jet mode is associated with the lowest nominal flow rate it is possible to obtain stable electrospray, the lowest value of $Q_{1(on)}$ will indeed be the same as $Q_{1(min)}$. $Q_{1(min)}$ is a special case of $Q_{1(on)}$ tested at the lowest possible nominal flow rate. There will then be further values of $Q_{1(on)}$ each associated with higher nominal flow rates. The onset flow rates for a multi-jet mode are then simply obtained to be the flow rate observed at the lowest voltage for a particular nominal flow rate that results in a particular multi-jet mode. As before, we anticipate that the total flow is equally divided between the number of jets observed and hence we assume that for example $Q_{2(on)}^{total}/2 = Q_{2(on)}$ is indicative of the flow rate through each jet in 2-jet mode. For simplicity we identify the onset flow rate per jet $Q_{n(on)}$ for n-jet mode. Thus for a particular experiment we can follow through the flow rate and current to provide values of $Q_{1(on)}$, $Q_{2(on)}$, $Q_{3(on)}$, etc.

Stable electrospray in PC1 across cone-jet and multi-jet modes was observed for a nominal flow rate between 3.0 nl/s and 120.3 nl/s. The associated values of $Q_{1(on)}$ varied over the range 7.3–125.5 nl/s. For each individual experiment (i.e. for a constant nominal flow rate) the ratio $Q_{2(on)}$:$Q_{1(on)}$ was determined together with similar ratios of flow rates per jet for 3 jets and 4 jets. The mean values for these ratios together with the standard deviation for the approximately 150 data sets are provided in Table 4.

We note that the ratios for $Q_{n+1(\mathrm{on})}/Q_{n(\mathrm{on})}$ as indicated in Table 4 approximately match the ratio of the increase in the number of jets, i.e. 1 to 2 jets onset flow is reduced by a factor of $\sim$1/2, in going from 2 to 3 jets there is a reduction by a factor of $\sim$2/3 etc. In Table 4 the corresponding ratios for minimum flow rate are also included, from which it is clear that the reduction in *minimum* flow is not simply associated with the increasing number of jets.

For each *n*-jet mode there is a flow rate range in which the electrospray is stable. To establish the relative stability of these modes, it is appropriate to non-dimensionalize the stability range by normalizing the flow rate range in a particular *n*-jet mode to that in single cone-jet mode. The normalized flow rate range for a particular *n*-jet mode is thus $Q_{n(range)}$ given by

$$Q_{n(range)} = \frac{(Q_{n(\max)} - Q_{n(\min)})}{(Q_{1(\max)} - Q_{1(\min)})} \tag{5}$$

and $Q_{n(max)}$ and $Q_{n(min)}$ are derived from the maximum total flow rate.

Eq. (5) is used to calculate the stable flow rate range experienced by each separate cone-jet system in the multi-jet mode. The results are plotted in Fig. 8. As anticipated from Fig. 6, the stable flow rate range for a particular jet mode reduces as the number of jets increases. In the propylene carbonate solution this reduction has a near linear dependence, with a similar trend in the TEG solutions. The observations presented in this way provide confirmation of the earlier identification of a maximum total electrospray flow rate, independently of the number of jets that are formed, since this will inevitably lead to a narrower range for the subsets of multi-jet mode involving a large number of jets.

In constant pressure fed electrospray systems operating in single cone-jet mode, as here, the flow rate increases as the applied voltage increases (Smith et al., 2006b). As a result the observed reduction in the stable flow rate, would suggest that the voltage range over which each multi-jet mode is stable will also be reduced; this indeed is observed. The external diameter of the electrospray emitter affects both the onset voltage in cone-jet mode (Smith, 1986) and the relationship between applied voltage and flow rate (Ryan et al., 2009). Therefore in order to gain further insight into the underlying issue of mode stability, it is important to identify those features which are associated with the size of the capillary, and those that are fundamentally electrohydrodynamic in nature. The electric field experienced by the fluid meniscus is related to both the voltage applied and the diameter of the capillary; in part this will lead to a factor of order the inverse square root of the diameter, however as the diameter changes the distance between the meniscus and the counter electrode also

Table 4
Normalized onset flow rate range ratio values in PC1.

	$Q_{2(on)}/Q_{1(on)}$	$Q_{3(on)}/Q_{2(on)}$	$Q_{4(on)}/Q_{3(on)}$
Mean	0.57	0.68	0.76
Standard deviation	0.09	0.02	0.01
	$Q_{2(min)}/Q_{1(min)}$	$Q_{3(min)}/Q_{2(min)}$	$Q_{4(min)}/Q_{3(min)}$
From Table 2	0.94	0.84	0.90

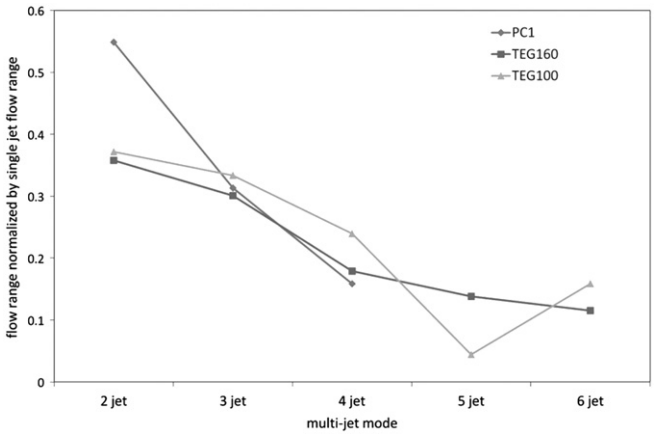

Fig. 8. Observed reduction in flow rate range $Q_{n(\mathrm{range})}$ with number of observed jets.

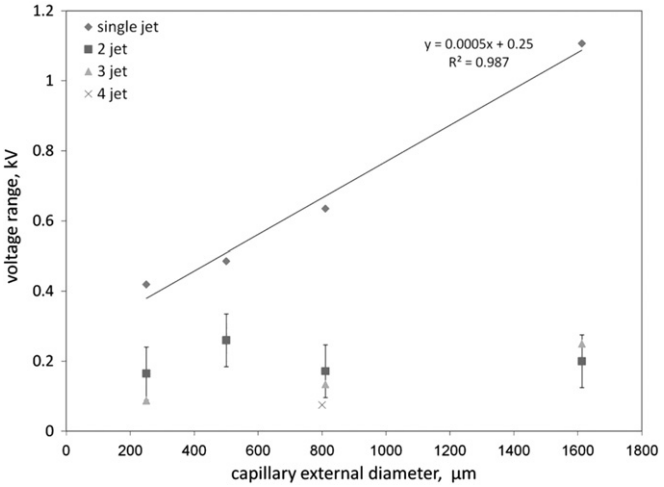

Fig. 9. Stable voltage range observed with PC1 solution during multi-jet operation.

changes, providing further complication to a direct comparison between (computed) electric field and stability range. In Fig. 9 the electrodynamic effects have therefore been highlighted by plotting the voltage range (rather than electric field range) over which a jet mode is stable as a function of the external diameter of the capillary.

It is apparent from this figure that in single cone jet mode the stability range as defined by the change in applied voltage for which this mode is stable, is dependent upon the diameter of the capillary, with a high regression coefficient for a linear relationship. However for the higher modes investigated, the influence of the external diameter seems minimal. For these higher jet modes ($n>1$) the stable voltage range has an average value across the modes of $\sim 0.17 \pm 0.07$ kV. This corresponds to an increase in voltage of only $\sim$4% relative to the average onset voltage for 2-jet mode electrospray. This therefore is indicative of the increased electric field required to develop an additional cone-jet structure on the pre-stressed conical meniscus, seemingly independent of both the number of existing jets and the capillary diameter. It is also suggestive that local to the forming instability, in going to jet modes with $n>1$, the effect of the other already existing jets only has a minor effect in terms of the field increase, in the region where the instability is forming.

4. Discussion of results

The observation that the relationship between current and flow rate appears to be the same in each multi-jet mode is certainly of interest and may provide an underlying process in electrospray experiments that has not been fully elucidated previously.

Duby et al. (2006) found that it is difficult to stabilize low flow rates in multi-jet, and for this reason they adopted a geometric feature to provide an attachment point for the multi-jet emission. It is not certain why in contrast we did not experience difficulty in obtaining stable low flow rate operation and importantly in our multi-jet system the flow rate per jet is also stable below $Q_{\min}$. We would note that our fluids are more than an order of magnitude higher conductivity than those of Duby et al., reducing the theoretical $Q_{\min}$. Thus our experiments observed stable flow substantially below those attempted in Duby's work. In order to achieve the lowest flow rate in our configuration, system hydraulic impedance is crucial, with high impedance aiding the attainment of low flow rate. In Duby's configuration the use of a syringe pump makes the operation rather different as the electrospray is not able to self-adjust flow rate to the changing electrostatic configuration, and in this may lie the underlying mechanism for our more stable operation.

Each of the solutions we have tested is of a relatively simple nature, namely that with regard to the charge availability in solution, this is likely only to result from charge separation of the salt NaI, dissolved in each solvent. The solvents, triethylene glycol and propylene carbonate may be assumed not to contribute ions to any measured current. This is unlike aqueous solutions wherein there is a potential contribution from other ions to net ionic conduction; in H_2O this could potentially be for example from hydronium ions. The metal capillaries that we used in these experiments were stainless steel; again under the conditions pertaining, it is less likely for the oxidation of metal ions to be released into solution. As a result it is possible to consider the measured current dependence on flow rate, as indicated in Figs. 5 and 6, to be the relationship of how efficiently ions are transferred from the solution with changing flow rate; this is the electrospray charge transfer efficiency η_{charge}. In this we are trying to provide further elucidation of the issue, highlighted in (Fernández de la Mora, 2007), Eq. (37) in comparing the current actually extracted from solution in comparison to the maximum charge available, $n_i eQ$, where n_i is the positive, or negative ion concentration, e is the charge per ion and Q the flow rate. Since the salt we have adopted in these experiments decomposes with a single net charge transfer it is unambiguous to

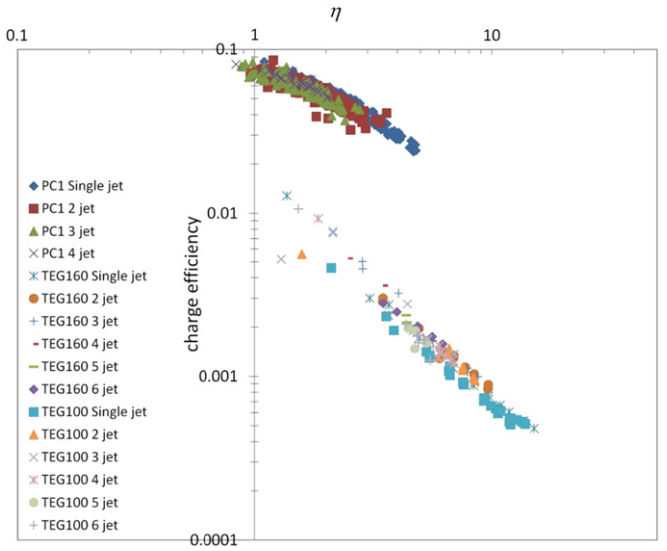

Fig. 10. Multi-jet ($n_{jet}=1$–6) charge efficiency, η_{charge} as a function of flow rate for solutions PC1 and TEG160.

identify the maximum available charge. As a result we define η_{charge} to be

$$\eta_{charge} = I/n_i eQ \tag{6}$$

Both in (Fernández de la Mora, 2007) and other publications (Higuera, 2009) there is recognition that minimum flow may be associated with complete charge separation of the available solution species, resulting in insufficient charge availability to maintain the electrospray system.

Fig. 10 is a plot of the measured value of η_{charge} for two of the fluids PC1 and TEG160 that we have tested as a function of non-dimensional flow rate. In this figure all the jet modes, including single jet are included and identified.

The individual data sets in each case are well captured (regression coefficients of 0.94–0.98) by a power law dependence of efficiency upon flow rate. This in itself is hardly surprising, given the data plotted in Fig. 6 since to within a constant factor, depending upon the fluid used

$$I \propto Q^{\alpha} \tag{7}$$

and from Eq. (3) therefore

$$\eta_{charge} \propto Q^{\alpha-1} \tag{8}$$

The best fitting power law exponent varies for the different fluids with α having the value of 0.60 for PC1 whereas it is 0.33 for TEG160.

As observed by other authors for single cone-jet mode, in multi-jet mode the value for η_{charge} increases as the flow rate approaches the minimum stable flow rate (Fernández de la Mora, 2007). We have noted in Section 3.2 that in multi-jet one is able to achieve a stable flow rate that is below the minimum stable flow rate observed in single jet, and significantly below the dimensionless flow rate $\eta=1$. At the even lower minimum flow rate noted in multi-jet mode, the charge efficiency continues to increase in the two solutions, but is however still well below full charge extraction as a result of salt dissociation with values of η_{charge} being 7.9% in PC1 and 1.3% for TEG160. Clearly in these moderately polar solvents the minimum flow rate for stable electrospray is not associated with charge extraction efficiency.

As shown in Fig. 3 there is a significant jump in current, whether or not this is associated with any change in total flow through the meniscus feeding the multiple jets, as the mode changes from n jets to $n+1$ jets. This suggests that at a flow rate well beyond the minimum flow rate and is approaching the condition for multi-jet mode, driven by the increasing value of electric field, there is already potentially available sufficient ion number density to support a higher current than is actually being extracted as net charge from the jet, without the requirement for any further increase in flow rate. This excess net charge is then able to support the current demanded by the additional jet, with all jets then established operating at the higher charge efficiency typified by the onset condition for the particular nominal flow rate in a given experiment. Thus there appears to be sufficient ion number density to support the higher current required for multi-jet operation, the issue is the ability to achieve a net anion/ cation species separation, in the vicinity of the n-jet transition region.

The ratio of total onset current, $I^{total}_{n(on)}$, measured at the lowest voltage after the mode was established to the total current measured immediately before mode change $I^{total}_{n-1(\max)}$ (i.e. maximum current in the previous mode) was evaluated. In the propylene carbonate fluid this ratio $I^{total}_{n(on)}/I^{total}_{n-1(\max)}$ had values of 1.29 ± 0.11 for the transition from 1 to 2 jets, 1.14 ± 0.05 for 2 to 3 jets 1.21 ± 0.55 for 3 to 4 jets. This increasing total current was associated with the current *per jet* always

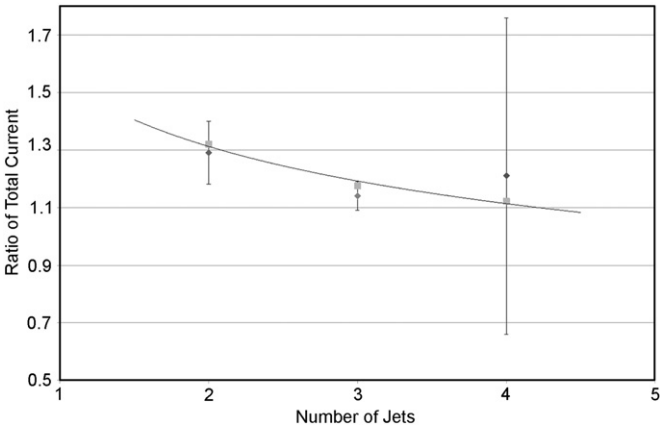

Fig. 11. Observed ratio $I^{total}_{n(on)}/I^{total}_{n-1(\max)}$ as a function of number of jets observed (diamond symbols with error bars) and ratio as predicted by Eq. (9) (square symbols), with trend line shown.

decreasing. We also note that the total flow rate is nominally constant during the jet mode transition from mode $(n-1)$ to (n) ie $Q^{total}_{n-1(\max)} \approx Q^{total}_{n(on)}$. The current for the onset of the 2 jet-mode, $I_{2(on)}$ was marked by a reduction in the maximum current from the single jet $I_{1(max)}$ by 35% with the two new jets appearing at the new onset current value $I_{2(on)}$. As the current in these two jets then reached their maximum stable value there was reduction of the current per jet in the mode change to 3 new jets of 24%. The similar transition to 4 jets was marked by a 9% drop in current for each jet. Evidently as the number of jets is increasing the reduction from the maximum current per jet to the onset current per jet, becomes less significant. Indeed this trend in the observations is well captured with a linear relationship, with a regression coefficient of 0.99. On the basis of the best-fit trend there would be no reduction in the current carried per jet as the number of jets increased to 5 (the actual intercept is for a jet number of 4.7). This suggests that there may be an underlying reason associated with the available charge, limiting the number of jets that can be stably sprayed in multi-jet, in the experimental configuration adopted here.

There is no strong statistical justification for the observed values of total current ratio $I^{total}_{n(on)}/I^{total}_{n-1(\max)}$ being other than having a single mean value of 1.24 (the deviation of any individual value about the mean for the values observed is less than 1.5σ). However, if we note that the total flow rate does not change significantly during the mode transition, as may be seen from Fig. 11, there appears to be a suggestive correlation between the observed current ratios when the measurement errors are included, and what would be predicted on the basis that each jet is indeed behaving in a similar manner. This predicted value of current ratio follows from Eqs. (4) and (7) from which one can write

$$I^{total}_{n}/I^{total}_{(n-1)} = (n/n-1)^{1-\alpha} \tag{9}$$

The trend provided by Eq. (9) identifies two features: (i) for large n the current ratio will tend to unity and (ii) the ratio will be dependent upon the exponent α, with larger values of α leading to a current ratio closer to unity at smaller values of n. In all experiments undertaken there was an increase in total current as an additional jet was observed to arise following an increase in voltage. For the TEG solutions, both of which had similar values of exponent α of $\sim$0.33, the maximum number of jets observed was 6, although several experiments were observed with 7 jets, but none with 8 jets. For the propylene carbonate solution with exponent α of 0.6 stable spray was only achieved with 4 jets, although a single experiment with 5 jets was noted. Thus on this basis, the dependence on α and the assumption that as the total current ratio approaches unity there is less likely to be additional jets being obtained, Eq. (9) provides the correct trend. Using the derived values of α in the solutions, in PC1 for 5 jets Eq. (9) gives a value of 1.09; in TEG160 Eq. (9) for 7 jets yields 1.11 and for 8 jets 1.09. In the case of PC1 the projected decrease in the observed current per jet from the maximum value in mode $n-1$ to the minimum current per jet in mode n noted above, is also consistent with a lack of stability for $\sim$5 jets.

This suggests that Eq. (9) can be used to identify the likely maximum number of jets that can be stably observed from a single meniscus. We emphasize that this limit is associated with the configuration studied here wherein there are no mechanical features used to enhance the stability of multi-jet operation, as clearly when such features are present then it is possible to obtain very many more multi-jets.

5. Conclusions

The multi-jet phenomenon studied here has a topology that includes a similar meniscus to the classic Taylor cone, from which normally only a single jet is apparent, particularly in the case where 2 jets are observed. As the number of jets increases the multi-jet phenomenon becomes the rim-jet phenomenon. Under the conditions we have investigated it appears that such a meniscus can maintain multiple jets wherein each jet mode has the same current dependence on flow rate independently of the number of jets observed. These observations supported by the other evidence provided here

strongly suggests that control of current flow is being obtained in the region immediately adjacent to the jet emanation from the large meniscus, that is in the transition region itself. Evidently in the multi-jet mode a number of local Taylor cone-jet structures must be formed, self similar to that for a single cone. The charge transfer efficiency for the moderately polar fluids studied here was low and as a result the minimum stable flow rate is unlikely to be associated with a failure of charge transfer. Minimum stable flow rates in multi-jet mode were observed to be systematically lower than their single cone-jet counterparts. The data we have obtained also indicates that there is a maximum number of jets that can be supported (in the absence of any physical rim type structures that may be used to impose multi-jet phenomena) in multi-jet, the value of this also relating to the minimum stable current that can be electrosprayed in a multi-jet system.

References

Alexander, M., Stark, S., Smith, J.P.W., Stevens, K.L., & Kent, B. (2006). Electrospray performance of microfabricated colloid thruster arrays. *Journal of Propulsion and Power*, *22*, 620–627.

Alexander, M.S., Smith, K.L., Paine, M.D., & Stark, J.P.W. (2007). Voltage-modulated flow rate for precise thrust control in colloid electrospray propulsion. *Journal of Propulsion and Power*, *23*, 1042–1048.

Aplin, K.L., Smith, K.L., Firth, J.G., Kent, B.J., Alexander, M.S., & Stark, J.P.W. (2008). Inexpensive optically isolated nanoammeter for use with micro-Newton electric propulsion technology. *Journal of Propulsion and Power*, *24*, 892–895.

Beyer, K., Bergfeld, W., Berndt, W., Carlton, W., Hoffmann, D., Schroeter, A., & Shank, R. (1987). Final report on the safety assessment of propylene carbonate. *International Journal of Toxicology*, *6*, 23–51.

Cloupeau, M., & Prunet-Foch, B. (1989). Electrostatic spraying of liquids in cone-jet mode. *Journal of Electrostatics*, *22*, 135–159.

Cloupeau, M., & Prunet-Foch, B. (1994). Electrohydrodynamic spraying functioning modes: a critical review. *Journal of Aerosol Science*, *25*, 1021–1036.

Duby, M.-H., Deng, W., Kim, K., Gomez, T., & Gomez, A. (2006). Stabilization of monodisperse electrosprays in the multi-jet mode via electric field enhancement. *Journal of Aerosol Science*, *37*, 306–322.

Fernández de la Mora, J. (2007). The fluid dynamics of Taylor cones. *Annual Review of Fluid Mechanics*, *39*, 217–243.

Fernández de la Mora, J., & Loscertales, I.G. (1994). The current emitted by highly conducting Taylor cones. *Journal of Fluid Mechanics*, *260*, 155–184.

Gamero-Castaño, M. (2001). Electrospray as a source of nanoparticles for efficient colloid thrusters. *Journal of Propulsion and Power*, *17*, 977–987.

Gañán-Calvo, A.M., Davila, J., & Barrero, A.J. (1997). Current and droplet size in the electrospraying of liquids. *Scaling laws Journal of Aerosol Science*, *28*, 249–275.

Gañán-Calvo, A.M. (2004). On the general scaling theory for electrospraying. *Journal of Fluid Mechanics*, *507*, 203–212.

Gu, W., et al. (2010). Generation of stable multi-jets by flow-limited field-injection electrostatic spraying and their control via I–V characteristics. *Journal of Physics D: Applied Physics*, *43*, 492001.

Gu, W.H., Singh, R., & Kim, K. (2005). Flow-limited field-injection electrostatic spraying for controlled formation of charged multiple jets of precursor solutions: theory and application. *Applied Physics Letters*, 87.

Hayati, I., Bailey, A., & Tadros, T.F. (1987). Investigations into the mechanism of electrohydrodynamic spraying of liquids: II. Mechanism of stable jet formation and electrical forces acting on a liquid cone. *Journal of Colloid and Interface Science*, *117*, 222–230.

Hendricks, C.D.J., Carson, R.S., Hogan, J.J., & Schneider, J.M. (1964). *AIAA Journal*, *2*, 722–737.

Higuera, F.J. (2009). Charge separation in the conical meniscus of an electrospray of a very polar liquid: its effect on the minimum flow rate. *Physics of Fluids*, *21*, 032104.

Jaworek, A., & Krupa, A. (1996). Forms of the multijet mode of electrohydrodynamic spraying. *Journal of Aerosol Science*, *27*, 979–986.

Jones, A.R., & Thong, K.C. (1971). The production of charged monodisperse fuel droplets by electrical dispersion. *Journal of Physics D: Applied Physics*, *4*, 1159–1168.

Juraschek, R., & Röllgen, F.W. (1998). Pulsation phenomena during electrospray ionization. *International Journal of Mass Spectrometry*, *177*, 1–15.

Kebarle, P., & Verkerk, U.H. (2009). Electrospray: from ions in solution to ions in the gas phase, what we know now. *Mass Spectrometry Reviews*, *28*, 898–917.

Lüttgens, U., Dülcks, T., & Röllgen, F.W. (1992). Field induced disintegration of glycerol solutions under vacuum and atmospheric pressure conditions studied by optical microscopy and mass spectrometry. *Surface Science*, *266*, 197–203.

Marsh, J.F., Nunn, A.E.T., & Michelson, D. (1988). The control of electrostatic atomization using a closed-loop system. *Journal of Electrostatics*, *20*, 313–318.

Martinez-Sanchez, M., & Pollard, J.E. (1998). Spacecraft electric propulsion—an overview. *Journal of Propulsion and Power*, *14*, 688–699.

Naejus, R., Lemordant, D., Coudert, R., & Willmann, P. (1997). Excess thermodynamic properties of binary mixtures containing linear or cyclic carbonates as solvents at the temperatures 298.15 K and 315.15 K. *The Journal of Chemical Thermodynamics*, *29*, 1503–1515.

Noymer, P.D., & Garel, M. (2000). Stability and atomization characteristics of electrodynamic jets in the cone-jet and multi-jet modes. *Journal of Aerosol Science*, *31*, 1165–1172.

Paine, M.D., Alexander, M.S., Smith, K.L., Wang, M., & Stark, J.P.W. (2007). Controlled electrospray pulsation for deposition of femtoliter fluid droplets onto surfaces. *Journal of Aerosol Science*, *38*, 315–324.

Park, I., Kim, W., & Kim, S.S. (2011). Multi-jet mode electrospray for non-conducting fluids using two fluids and a coaxial grooved nozzle. *Aerosol Science and Technology*, *45*(5), 629–634.

Rayleigh, L. (1882). On the equilibrium of liquid conducting masses charged with electricity. *Philosophical Magazine Series*, *5*(14), 184–186.

Riddick, J.A., Bunger, W.B., & Sakano, T.K. (1986). *Organic solvents: physical properties and methods of purification* (4th ed.). Wiley-Interscience: .

Ryan, C.N. (2010). Influence of electrostatics upon electrospray with the intention of application to colloid thrusters. Ph.D., Queen Mary University of London, London Unpublished.

Ryan, C.N., Smith, K.L., Alexander, M.S., & Stark, J.P.W. (2009). Effect of emitter geometry on flow rate sensitivity to voltage in cone jet mode electrospray. *Journal of Physics D: Applied Physics*, *42*, 155504.

Shtern, V., & Barrero, A. (1994). Striking features of fluid flows in taylor cones related to electrosprays. *Journal of Aerosol Science*, *25*, 1049–1063.

Smith, D.P.H. (1986). The electrohydrodynamic atomization of liquids. *IEEE Transactions on Industry Applications*, *IA-22*, 527–535.

Smith, K.L. (2005). *Characterisation of electrospray properties in high vacuum: with a view to application in colloid thruster technology.* Ph.D., Queen Mary University of London, London Unpublished.

Smith, K.L., Alexander, M.S., & Stark, J.P.W. (2006a). The role of molar conductivity in electrospray cone-jet mode current scaling. *Journal of Applied Physics*, *100*, 014905.

Smith, K.L., Alexander, M.S., & Stark, J.P.W. (2006b). The sensitivity of volumetric flow rate to applied voltage in cone-jet mode electrospray and the influence of solution properties and emitter geometry. *Physics of Fluids*, *18*, 092104.

Taylor, G. (1964). Disintegration of water drops in an electric field. *Proceedings of the Royal Society of London. Series A, Mathematical and Physical Sciences*, *280*, 383–397.

Thong, K.C., & Weinberg, F.J. (1971). Electrical control of the combustion of solid and liquid particulate suspensions. *Proceedings of the Royal Society of London. Series A, Mathematical and Physical Sciences*, *324*, 201–215.

Yoon, S.S., Heister, S.D., Epperson, J.T., & Sojka, P.E. (2001). Modeling multi-jet mode electrostatic atomization using boundary element methods. *Journal of Electrostatics*, *50*, 91–108.

Zeleny, B.A. (1915). On the conditions of instability of electrified drops, with applications to the electric discharge from liquid points. *Proceedings of the Cambridge Philosophical Society*, *18*, 71–83.
Zeleny, J. (1914). The electrical discharge from liquid points and a hydrostatic method of measuring the electric intensity at their surfaces. *The Physical Review*, 3, 69–91.
Zeleny, J. (1917). Instability of Electrified Liquid Surfaces. *The Physical Review*, *10*, 1–6.